



1 **Effects of CO₂ on the nitrogen isotopic composition of**

2 ***Trichodesmium and Crocosphaera***

3 ZuoZhu Wen^{1,*}, Ruotong Jiang^{1,*}, Tianli He¹, Thomas J. Browning², Haizheng Hong¹,

4 Dalin Shi¹

5

6 ¹*State Key Laboratory of Marine Environmental Science, Xiamen University; Xiamen,*

7 *PR China.*

8 ²*Marine Biogeochemistry Division, GEOMAR Helmholtz Centre for Ocean Research*

9 *Kiel; Kiel, Germany.*

10 **These authors contributed equally to this work.*

11

12 ***Correspondence:*** Dalin Shi (dshi@xmu.edu.cn)



13 **Abstract**

14 Biological nitrogen (N₂) fixation is the main input of fixed nitrogen to ecosystems on
15 Earth. Nitrogen isotope fractionation during this process is a key parameter for
16 understanding the nitrogen cycle, however, relatively little is known about its
17 regulatory mechanisms. Here we examine the effects of varying CO₂ concentrations
18 on biomass δ¹⁵N signatures of the cyanobacterial diazotrophs *Trichodesmium*
19 *erythraeum* and *Crocospaera watsonii*. We show that these organisms produce
20 biomass up to ~3‰ lower in δ¹⁵N under either decreased (~180 μatm) or elevated
21 (~1400 μatm) CO₂ concentrations in comparison to modern levels (~380 μatm). Our
22 results pointed towards changes in nitrogenase enzyme efficiency in response to CO₂
23 perturbations impacting isotopic fractionation during N₂ fixation and thus the biomass
24 δ¹⁵N. This study contributes to an improved interpretation of the observed fluctuations
25 in the δ¹⁵N records, and thus the past nitrogen cycle on Earth.

26



27 **1. Introduction**

28 Nitrogen fixation by diazotrophic bacteria converts abundant dinitrogen (N₂) gas into
29 ammonia, which sustains the oceanic N reservoir and thereby ocean productivity
30 (Stueken et al., 2015; Gruber and Galloway, 2008; Altabet, 2007). This process is
31 catalyzed by the metalloenzyme nitrogenase and produces organic N that is
32 isotopically depleted in ¹⁵N ($\delta^{15}\text{N}$, $[(^{15}\text{N}/^{14}\text{N}_{\text{sample}}/^{15}\text{N}/^{14}\text{N}_{\text{air}}) - 1] \times 1,000$ when
33 expressed in per mil) relative to source N₂. This is opposite to denitrification and
34 anammox, which return lighter N to the atmosphere, leaving the marine nitrate (NO₃⁻)
35 pool and resulting biomass relatively enriched in ¹⁵N (Casciotti, 2016; Brunner et al.,
36 2013). Therefore, the isotope effect of N₂ fixation (i.e., the fractionation factor for N₂
37 fixation, ϵ_{fix}) is a key parameter for isotope-based studies of present and past N
38 cycling on Earth (Lloyd et al., 2020; Casciotti, 2016).

39

40 The isotopic effect of N₂ fixation on nitrogen was traditionally assumed to be
41 invariant with environmental conditions and equivalent to the in vivo isotope effect
42 of molybdenum (Mo)-nitrogenase ($\epsilon_{\text{fix}}^{\text{Mo}}$ is $\sim +2\%$) (Carpenter et al., 1997;
43 Bauersachs et al., 2009; Minagawa and Wada, 1986). Researchers have therefore
44 often adopted a $\delta^{15}\text{N}$ value of $\sim -1\%$ for biomass produced by diazotrophs (Brandes
45 and Devol, 2002; Montoya, 2008; Sigman et al., 2009). Geologists have used N inputs
46 primarily from N₂ fixation and the subsequent recycling of ammonium from
47 diazotrophic biomass decay, to account for the low $\delta^{15}\text{N}$ values (centered around 0%)
48 found in ancient sediments dating back approximately 2.7 billion years (Gyr) (Lloyd



49 et al., 2020). However, the presence of extremely negative bulk $\delta^{15}\text{N}$ values ($< \sim -2\text{‰}$,
50 can low to -7‰) in the Cretaceous Oceanic Anoxic Events (OAEs, 145–66 Myr) and
51 the early Archean (>3.2 Gyr ago), which are not observed in modern marine
52 sediments (Altabet and Francois, 1994; Altabet, 2007; Shen et al., 2006), challenges
53 the current understanding of the marine nitrogen isotope budget (Brandes and Devol,
54 2002).

55

56 Until recently, studies have demonstrated that changes in environmental conditions
57 significantly impact the $\delta^{15}\text{N}$ values in diazotrophic biomass, providing new insights
58 into the variability of the $\delta^{15}\text{N}$ records. For instance, *Anabaena*, a filamentous
59 cyanobacterium, shows up to a 3‰ increase in $\delta^{15}\text{N}$ of biomass when grown in Fe-
60 limited versus Fe-enriched media (Zerkle et al., 2008), mainly due to the release of
61 isotopically lighter N in siderophores under Fe limitation (Mcrose et al., 2019).

62 Additionally, increased N_2 partial pressure in *Anabaena* cultures revealed that higher
63 pressures resulted in significantly lighter $\delta^{15}\text{N}$ biomass, although the difference was
64 relatively minor (less than 0.5‰) (Silverman et al., 2019). Additionally, a critical
65 discovery potentially explaining the extremely low $\delta^{15}\text{N}$ values in ancient sediments
66 was the use of vanadium (V-) and Fe-only alternative nitrogenases, which yield
67 significantly lower $\delta^{15}\text{N}$ biomass (-6 to -7‰) (Rowell et al., 1998; Zhang et al., 2014).

68 The mechanism by which the use of alternative nitrogenase enzymes alters isotope
69 fractionation remains unclear. Given the lower efficiency of the V- and Fe-only
70 nitrogenases compared to the Mo-nitrogenases (Eady, 1996; Miller and Eady, 1988),



71 it is possible that the commitment to N₂ catalysis is decreased due to 1) a decline in N₂
72 reduction efficiency post-binding to the active site; 2) or an increased competition at
73 the active site between N₂ and H₂ (Guth and Burris, 1983; Yang et al., 2013), with the
74 latter being more abundantly produced by alternative nitrogenases (Eady, 1996). The
75 decreased commitment to catalysis may thus lead to a more complete expression of
76 the isotopic effect associated with the subsequent N₂ bond-breaking step of the
77 nitrogenase catalyzation.

78

79 Recent studies show that ocean acidification resulting from elevated *p*CO₂ above the
80 modern levels (~380 μatm vs. ~800 μatm) significantly reduces the efficiency of Mo-
81 nitrogenase in the filamentous diazotrophic cyanobacterium *Trichodesmium* (Shi et
82 al., 2012; Hong et al., 2017; Zhang et al., 2019; Zhang et al., 2022). This is probably
83 attributed to a greater allocation of electrons to protons (H⁺) rather than N₂ at low pH
84 (8.1 vs. 7.8), as evidenced by an enhanced production of H₂ (Shi et al., 2012; Pham
85 and Burgess, 1993). Should this phenomenon be consistent across all diazotroph
86 species and nitrogenase types, past fluctuations in atmospheric CO₂ [which exceeded
87 1500 ppm prior to 420 Myr, dropping to pre-industrial levels (ca. 280 ppm) after ~20
88 Myr (Fig. S1)] might have notably impacted nitrogenase efficiency, and consequently,
89 the isotopic fractionation during N₂ fixation. Here we examine the effect of changing
90 CO₂ concentrations on biomass δ¹⁵N of model cyanobacterial diazotrophs
91 *Trichodesmium erythraeum* IMS101 and *Crocospaera watsonii* WH8501. We
92 present the first evidence that changes in CO₂ levels significantly alter the biomass



93 $\delta^{15}\text{N}$ of both species by impacting nitrogenase efficiency. Our findings provide new
94 insights into the fluctuations observed in the $\delta^{15}\text{N}$ records, and thus the Earth's past
95 nitrogen cycle.

96 **2. Methods**

97 **2.1 Bacterial strains and culture conditions**

98 The marine cyanobacterium *Trichodesmium erythraeum* IMS101 and *Crocospaera*
99 *watsonii* WH8501 were grown in Aquil-tricho medium prepared with 0.22 μm -
100 filtered and microwave-sterilized oligotrophic South China Sea surface water (Hong
101 et al., 2017). Cultures underwent an acclimation period spanning at least 20
102 generations prior to starting the experiments. The medium was enriched with 10 μM
103 chelexed (cation exchange resin) and filter-sterilized NaH_2PO_4 , filter-sterilized
104 vitamins and trace metals buffered with 20 μM EDTA (Sunda et al., 2005), and a
105 replete concentration of Fe (1 μM). Cultures were unialgal and grown under five
106 $p\text{CO}_2/\text{pH}$ (~180 to 1400 μatm , pH ~7.5 to 8.3) conditions at 27°C and 80 μmol
107 photons $\text{m}^{-2} \text{s}^{-1}$ (14 h: 10 h light–dark cycle) in an AL-41L4 algae chamber
108 (Percival). The experimental $p\text{CO}_2/\text{pH}$ was chosen to fall within the range in the last
109 420 million years (Fig. S1) (Foster et al., 2017). All experiments were carried out with
110 three biological replicates. Sterile techniques were applied for culturing and
111 experimental manipulations. All data of the measured parameters including carbonate
112 chemistry, growth and N_2 fixation rates, biomass $\delta^{15}\text{N}$, and nitrogenase efficiency are
113 shown in Table S1 and supplementary data.



114

115 **2.2 Carbonate chemistry manipulation**

116 $p\text{CO}_2$ /pH in media was manipulated by adding different amounts of ultra-pure HCl
117 and NaOH (both from Sigma-Aldrich Chemical) (Shi et al., 2009). The pH of media
118 was monitored daily for *Trichodesmium* and every two days for *Crocospaera*, using
119 a spectrophotometric method (Zhang and Byrne, 1996) and each manipulated pH
120 remained stable throughout the experimental period (Fig. S2). The dissolved inorganic
121 carbon (DIC) concentration was analyzed using a CO_2 analyzer (LI 7000, Apollo
122 SciTech). Calculations of alkalinity and $p\text{CO}_2$ were made using the CO2Sys program
123 (Pierrot et al., 2011).

124

125 **2.3 Chla, cell concentrations and growth rate**

126 The growth of *Trichodesmium* was monitored by measuring Chla concentrations
127 daily, while the growth of *Crocospaera* was monitored through the measurement of
128 cell abundance every two days. *Trichodesmium* Chla concentration was determined
129 via extraction in 90% methanol, followed by analysis using a spectrophotometer
130 according to De Marsac and Houmard (1988). *Crocospaera* cell densities
131 were determined using a Z2 Coulter Counter (Beckman Coulter). Specific growth
132 rates were calculated from linear regressions of the natural logarithm of Chla or cell
133 concentration vs. time for the exponential growth phase and four data points were
134 included in each growth curve.

135



136 **2.4 N₂ fixation rates and δ¹⁵N signal of biomass**

137 N₂ fixation rates were measured using the ¹⁵N₂ gas dissolution method (Mohr et al.,
138 2010). Briefly, ¹⁵N₂ enriched water was prepared according to Wen et al. (2022) by
139 fully dissolving 5 mL 98% pure ¹⁵N₂ gas (Cambridge Isotope Laboratories) into 500
140 mL degassed seawater. After that, 25 mL ¹⁵N₂-enriched water was added to each 250
141 mL polycarbonate bottle containing diazotroph culture, and then incubated at the
142 same culture conditions for 2 h. The measurement was conducted at the midpoint of
143 the light period and dark period, respectively, for *Trichodesmium* and *Crocospaera*.
144 After incubation, diazotrophs were filtered onto 25 mm pre-combusted GF/F filters
145 (Millipore). Diazotrophs were collected by filtration concurrently with the N₂ fixation
146 rate measurement, but not enriched with ¹⁵N₂, to determine the natural biomass δ¹⁵N
147 signal. All filter samples were then dried and analyzed using a Thermo Scientific
148 Flash 2000 HT elemental analyzer coupled with a Thermo Finnigan Deltaplus
149 Advantage isotope ratio mass spectrometer. The N₂ fixation rate was calculated
150 according to Montoya et al. (1996).

151

152 **2.5 Quantification of *NifH* proteins**

153 *Trichodesmium* and *Crocospaera* cells were collected onto polycarbonate membrane
154 filters (Millipore) at the midpoint of the light and dark period respectively. Proteins
155 were extracted and denatured in an extraction buffer (50 mM Tris–HCl pH 6.8, 2%
156 w/v SDS, 10% v/v glycerol, and 1% v/v β-mercaptoethanol) under heating at 100 °C
157 for 10 min, followed by centrifugation at 20,000 g for 5 min to remove insoluble



158 material. Total protein in the supernatant was measured using the bicinchoninic acid
159 (BCA) assay (Thermo Fisher Scientific, California, USA). Equal amounts of proteins
160 were separated on a 12% sodium dodecyl sulfate-polyacrylamide gel (SDS-PAGE) for
161 30 min at 200 V. Proteins were transferred to a PVDF membrane in ice-cold transfer
162 buffer [25 mM Tris, 192 mM glycine, and 2.5% (vol/vol) methanol]. The membrane
163 was blocked with 5% milk powder in TBST buffer [Tris-buffered saline containing
164 0.25% (vol/vol) Tween-20, pH 7.5] for 1 h. Then, the membrane was incubated for 1
165 h with primary antibodies (Agrisera: NifH, Art no. AS01 021S), followed by 1 h
166 incubation with Goat anti Chicken IgY (Agrisera: Art no. AS09 606) with TBST
167 washes before and after. The membrane then was probed with alkaline phosphatase
168 (AP stock solution, pH 9.5), and visualized with NBT/BCIP (Roche, Indianapolis).
169 Protein bands were quantified by densitometry and protein levels were calculated
170 from the standard (Agrisera: NifH, Art no. AS01 021S) curves.

171

172 **2.6 Statistical analysis**

173 Data was analyzed using MATLAB R2022b to determine the statistical significance
174 of differences via either t-test or one-way ANOVA. A significance level of $p < 0.05$
175 was applied.

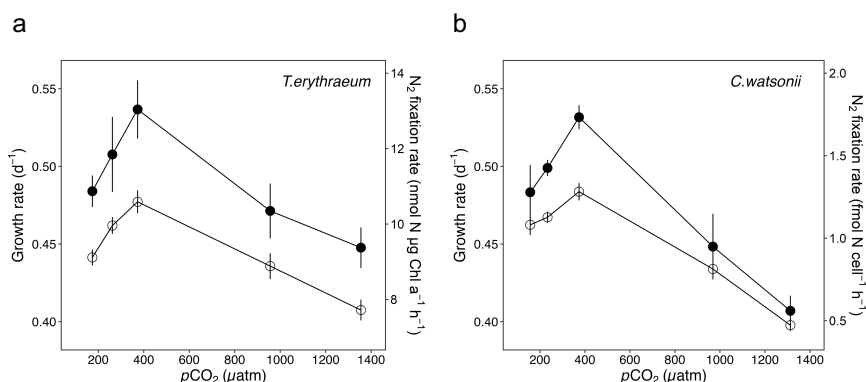
176

177 **3. Results and discussion**

178 **3.1 Growth and N₂ fixation rates response to CO₂ perturbations**



179 In our study, *Trichodesmium* and *Crocospaera* were cultivated under a range of
180 $p\text{CO}_2/\text{pH}$ conditions, with $p\text{CO}_2$ varying from approximately ~ 180 to $1400 \mu\text{atm}$ and
181 pH levels ranging from about 7.5 to 8.3. These conditions were selected to reflect the
182 environmental variability over the past 420 million years (Fig. S1), as outlined in
183 Foster et al. (2017). N_2 served as the sole nitrogen source for these organisms. The
184 growth and N_2 fixation rates exhibited by both species varied markedly across the
185 different $p\text{CO}_2$ levels, displaying a unimodal-like response to $p\text{CO}_2$ perturbations
186 (Fig. 1). Notably, these rates were at their peak under modern $p\text{CO}_2$ levels (~ 380
187 μatm) and decreased significantly at both lower and higher $p\text{CO}_2$ concentrations.
188



189
190 **Figure 1. Growth and N_2 fixation rates of *T. erythraeum* (a) and *C. watonii* (b) in**
191 **response to CO_2 perturbations.** Filled dots stand for growth rate; The open circles
192 are N_2 fixation rates. Note that N_2 fixation rates of *Trichodesmium* and *Crocospaera*
193 are measured in different units. The values of growth rates and N_2 fixation rates are
194 presented as mean \pm SD ($n = 3$).

195

196 The response of phytoplankton to CO_2 perturbations lies in the simultaneous changes

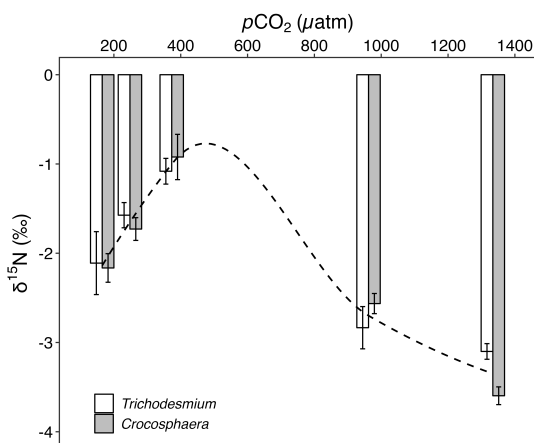
197 in $p\text{CO}_2$ and pH, which can have conflicting effects on their physiology and growth.



198 For instance, the C-fixing enzyme RubisCO of cyanobacteria (including
199 *Trichodesmium* and *Crocospaera*) generally has a half-saturation concentration an
200 order of magnitude higher ($> 100 \mu\text{M}$) than the current seawater CO_2 level ($\sim 10 \mu\text{M}$)
201 (Badger et al., 1998). This forces them to invest substantial resources and energy into
202 carbon concentration mechanisms (CCMs) to increase intracellular CO_2 , particularly
203 at low seawater $p\text{CO}_2$ levels (e.g. $\sim 180 \mu\text{atm}$). Elevated environmental CO_2
204 concentrations are expected to downregulate CCMs, and thus benefit cell growth and
205 N_2 fixation (Kranz et al., 2011; Badger et al., 2006). Conversely, the concurrent
206 decrease in seawater pH may significantly reduce the cytosolic pH and nitrogenase
207 efficiency, and thus the growth and N_2 fixation rates (Hong et al., 2017). Given that
208 the cytosolic pH of *Trichodesmium* is about 1 unit lower than its environmental
209 conditions as previously reported by Hong et al. (2017), and assuming a similar
210 condition of *Crocospaera*, the elevated CO_2 levels from ~ 180 to $1400 \mu\text{atm}$ may
211 decrease the cytosolic pH of both species to levels of ~ 7.3 to 6.5 , with two lowest pHs
212 (CO_2 levels ~ 1000 and $1400 \mu\text{atm}$) deviating from the optimal pH range (7–8) for
213 nitrogenase activity (Hadfield and Bulen, 1969; Imam and Eady, 1980; Schneider et
214 al., 1995; Pham and Burgess, 1993). Therefore, the observed increases in growth and
215 N_2 fixation rates from $\sim 180 \mu\text{atm}$ to modern CO_2 levels of $400 \mu\text{atm}$ (Fig. 1) indicate
216 an overall dominance of beneficial effects from elevated $p\text{CO}_2$, with minimal impact
217 from reduced pH as the cytosolic pH is still within the optimal range. In contrast, the
218 substantial declines in growth and N_2 fixation at high CO_2 levels beyond the modern
219 levels (~ 1000 and $1400 \mu\text{atm}$, Fig. 1) reflects the detrimental impacts of reduced pH,



220 which outweigh the positive effects of elevated $p\text{CO}_2$.



221

222 **Figure 2. Biomass $\delta^{15}\text{N}$ values of *T. erythraeum* and *C. wastonii* produced when**
223 **grown in variable CO_2 concentrations. White, *Trichodesmium*; Grey,**
224 ***Crocosphaera*. The values of biomass $\delta^{15}\text{N}$ are presented as mean \pm SD ($n = 3$). The**
225 **dashed line is the overall trend of biomass $\delta^{15}\text{N}$ of both species in response to CO_2**
226 **perturbations.**

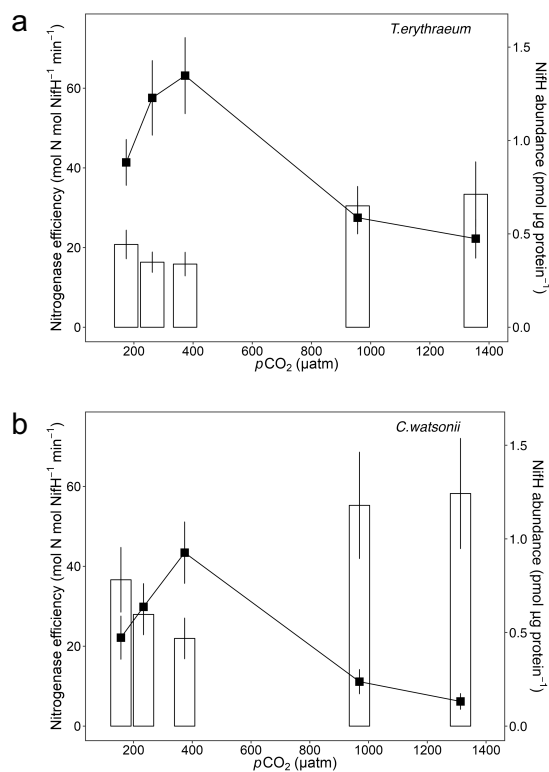
227

228 3.2 Biomass $\delta^{15}\text{N}$ responses to CO_2 perturbations

229 The biomass $\delta^{15}\text{N}$ of both *Trichodesmium* and *Crocosphaera* exhibit a response to
230 $p\text{CO}_2/\text{pH}$ perturbations that is analogous to their growth and N_2 fixation rates. Under
231 modern CO_2 conditions, the biomass $\delta^{15}\text{N}$ values peaked at around -1‰ for both
232 species (Fig. 2). These values align well within the range of -0.7 to -0.25‰ previously
233 reported for biomass produced by *Trichodesmium* collected from Sargasso Sea and
234 Caribbean Sea (Carpenter et al., 1997), and are also consistent with the biomass $\delta^{15}\text{N}$
235 values typically associated with organisms utilizing the 'canonical' Mo-nitrogenase
236 (Zhang et al., 2014). Our data reveal that any deviation from the modern $p\text{CO}_2$ levels,
237 either an increase or decrease, results in a significant reduction ($p < 0.01$, determined
238 by one-way ANOVA) in biomass $\delta^{15}\text{N}$. Specifically, at $\sim 1400 \mu\text{atm } p\text{CO}_2$, the



239 biomass $\delta^{15}\text{N}$ decreased by a maximum of 2.0‰ for *Trichodesmium* and 2.7‰ for
240 *Crocospaera*.
241
242 Our study shows for the first time that CO_2 exerts important controls on the N isotopic
243 composition of diazotrophic biomass. Additionally, we observed that both growth and
244 N_2 fixation rates were significantly positively correlated with biomass $\delta^{15}\text{N}$ (R^2 for
245 both species are higher than 0.9, $p < 0.05$, Fig. S3). The mechanisms behind these
246 strong correlations remain unclear. Regarding the mechanism behind the ocean
247 acidification effect on *Trichodesmium*, previous research has indicated that a decrease
248 in nitrogenase efficiency at elevated $p\text{CO}_2$ levels above 400 μatm , is a primary factor
249 leading to reduced growth and N_2 fixation rates (Hong et al., 2017; Shi et al., 2012).
250 Additionally, it has been inferred that changes in nitrogenase efficiency can also
251 impact isotopic fractionation during N_2 fixation. For instance, the lower efficiency of
252 alternative V- and Fe-only nitrogenases compared to the canonical Mo-nitrogenase
253 (Miller and Eady, 1988; Eady, 1996) is hypothesized to result in a more pronounced
254 isotopic effect during N_2 fixation, thereby leading to more negative $\delta^{15}\text{N}$ values in
255 biomass (Zhang et al., 2014). We thus hypothesize that the correlations of growth and
256 N_2 fixation rates with biomass $\delta^{15}\text{N}$ in our study, are mediated by nitrogenase
257 efficiency under CO_2 perturbation.



258

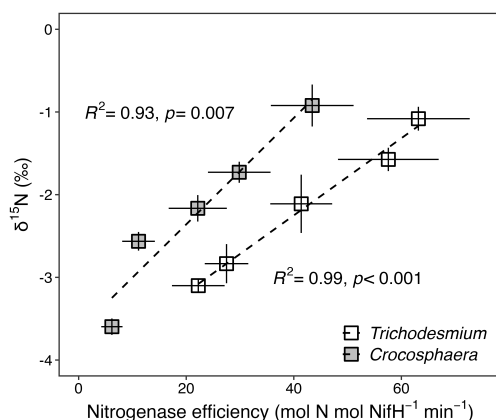
259 **Figure 3. Nitrogenase efficiency of *T. erythraeum* (a) and *C. watsonii* (b) in**
260 **response to CO_2 perturbations.** The filled squares stand for the nitrogenase
261 efficiency; The hollow bars are nitrogenase reductase (NifH) protein abundances.
262 Data shows the mean \pm standard deviation of $n = 3$ biological replicates.

263

264 We therefore calculated the nitrogenase efficiency of *Trichodesmium* and
265 *Crocospaera* by normalizing $^{15}\text{N}_2$ -based N_2 fixation rates to the abundance of
266 nitrogenase reductase (NifH) protein. In alignment with previous finding, we
267 observed significant reductions in nitrogenase efficiency for both species under
268 elevated CO_2 conditions (corresponding to decreased pH) above the modern levels (p
269 < 0.05 , One-way ANOVA, Fig. 3). This reduction was attributed to a decrease in N_2
270 fixation rates coupled with an increase in NifH protein production (Figs. 1 and 3). We



271 also noted a significant decrease in nitrogenase efficiency at $\sim 180 \mu\text{atm } p\text{CO}_2$
272 compared to modern $p\text{CO}_2$ levels ($p < 0.05$, One-way ANOVA, Fig. 3). As discussed
273 above, under low CO_2 concentrations ($< 380 \mu\text{atm}$), *Trichodesmium* and
274 *Crocospaera* will need to invest substantial resources and energy into CCMs
275 to enhance the efficiency of RubisCO carboxylation, thereby reducing the risk of
276 carbon limitation (Giordano et al., 2005; Badger et al., 2006; Kaplan and Reinhold,
277 1999). Enhanced expression of CCMs may thus divert energy and resources that
278 would otherwise be allocated to other cellular metabolic pathways, such as N_2 fixation
279 (Levitan et al., 2007; Kranz et al., 2009; Barcelos E Ramos et al., 2007). We therefore
280 hypothesize that CO_2 limitation may reduce energy and reductant supply to
281 nitrogenase and decrease the enzyme efficiency, though the mechanism remained
282 unsolved. Irrespective of the specific mechanisms driving variations in nitrogenase
283 efficiency, we found significant positive correlations between CO_2 -controlled
284 nitrogenase efficiency and biomass $\delta^{15}\text{N}$ ($R^2 = 0.99$, $p < 0.001$ and $R^2 = 0.93$, $p =$
285 0.007 for *Trichodesmium* and *Crocospaera* respectively, Fig. 4). Our results
286 therefore point towards the potential roles of nitrogenase efficiency in regulating the
287 kinetic isotopic effect of N_2 fixation.



288

289 **Figure 4. Relationships between nitrogenase efficiency and biomass $\delta^{15}\text{N}$.** Open

290 squares, *Trichodesmium*; Grey squares, *Crocosphaera*. Data shows the mean \pm

291 standard deviation of $n = 3$ biological replicates.

292

293 4. Conclusion and implications

294 Our research has established that CO_2 perturbation significantly affects the N isotopic

295 fractionation during cyanobacterial N_2 fixation. We observed significant ^{15}N -depleted

296 biomass in cyanobacterial diazotrophs grown under CO_2 concentrations either below

297 or above modern levels. These findings appear to be strongly linked to the efficiency

298 of nitrogenase. This study suggests a mechanism through which fluctuations in CO_2

299 could influence trends in $\delta^{15}\text{N}$ values preserved in ancient organic matter found in

300 sediments.

301

302 During glacial/interglacial cycles over the past 800,000 years (as illustrated in Fig.

303 S1), the periodic presence of lighter sediment $\delta^{15}\text{N}$ [as low as $\sim 2\text{--}4\%$ in the

304 (sub)tropical regions] during interglacial periods has been previously associated with



305 changes in upper water column structure, sea level, and ocean circulation, which lead
306 to the import of 'excess' phosphorus into the ocean surface and consequently enhance
307 N₂ fixation (Ren et al., 2009; Straub et al., 2013; Li et al., 2019). If our short-term
308 experimental observations are indicative of diazotroph growth patterns in the
309 geological past, it could be inferred that the elevated CO₂ levels during the interglacial
310 periods (rising from ~180 μatm to 300 μatm) might have resulted in 0.5 to 1‰ lesser
311 isotopic effect of Mo-nitrogenase and thus isotopically heavier N biomass by
312 cyanobacterial diazotrophs. This suggests that isotope-based study into the
313 contribution of N₂ fixation to the overall N inputs during glacial/interglacial periods
314 needs to take into account the impact of environmental changes on the isotopic
315 fractionation of N₂ fixation. Furthermore, prior to the Miocene epoch (> 20 million
316 years ago, as shown in Fig. S1), elevated CO₂ (up to ~ 5000 μatm at 201 Myr) above
317 modern levels (~380 μatm) (Hönisch et al., 2012) might have also led to the
318 production of isotopically lighter biomass. This could offer additional insights into the
319 anomalously low δ¹⁵N values (< -2‰) observed in sediments from the Oceanic
320 Anoxic Events of the Cretaceous period (145–66 Myr), suggesting that if extant
321 diazotrophs utilizing alternative nitrogenases during these periods responded similarly
322 to the changes in CO₂ as observed in our study, it could partly explain those low δ¹⁵N
323 sediment values (Lloyd et al., 2020).
324
325
326
327



328 **Data availability.** All data needed to evaluate the conclusions in the paper are present
329 in the paper and/or the Supplement. Additional data associated with the paper are
330 available from the corresponding authors upon request.

331

332 **Author contributions.** DS and HH designed the research. TH and ZW performed the
333 experiments. RJ, ZW, TH and DS analyzed the data. ZW, RJ, TJB and DS wrote the
334 manuscript. All authors discussed the results and commented and edited the
335 manuscript.

336

337 **Competing interests.** The authors declare that they have no conflict of interests.

338

339 **Acknowledgments.** We thank S.-J. Kao, W. Zou, and L. Tian for technical assistance
340 with the analysis of PON and its isotopic composition.

341

342 **Financial support.** This work was supported by the National Science Foundation of
343 China (41925026, 42076149 and 42106041), the National Key Research and
344 Development Program of China (2022YFE0136600 and 2023YFF0805000) and the
345 “111” Center (BP0719030). Dalin Shi was also supported by the New Cornerstone
346 Science Foundation through the XPLOER Prize.

347



348 References

- 349 Altabet, M. A.: Constraints on oceanic N balance/imbalance from sedimentary ¹⁵N
350 records, *Biogeosciences*, 4, 75-86, <https://doi.org/10.5194/bg-4-75-2007>, 2007.
- 351 Altabet, M. A. and Francois, R.: Sedimentary nitrogen isotopic ratio as a recorder for
352 surface ocean nitrate utilization, *Global Biogeochem. Cycles*, 8, 103-116,
353 <https://doi.org/10.1029/93GB03396>, 1994.
- 354 Badger, M. R., Price, G. D., Long, B. M., and Woodger, F. J.: The environmental
355 plasticity and ecological genomics of the cyanobacterial CO₂ concentrating mechanism,
356 *J. Exp. Bot.*, 57, 249-265, <https://doi.org/10.1093/jxb/eri286>, 2006.
- 357 Badger, M. R., Andrews, T. J., Whitney, S. M., Ludwig, M., Yellowlees, D. C., Leggat,
358 W., and Price, G. D.: The diversity and coevolution of Rubisco, plastids, pyrenoids, and
359 chloroplast-based CO₂-concentrating mechanisms in algae, *Can J Bot.*, 76, 1052-1071,
360 <https://doi.org/10.1139/b98-074>, 1998.
- 361 Barcelos e Ramos, J., Biswas, H., Schulz, K. G., LaRoche, J., and Riebesell, U.: Effect
362 of rising atmospheric carbon dioxide on the marine nitrogen fixer *Trichodesmium*,
363 *Global Biogeochem. Cycles*, 21, <https://doi.org/10.1029/2006gb002898>, 2007.
- 364 Bauersachs, T., Schouten, S., Compaoré, J., Wollenzien, U., Stal, L. J., and Sinninghe
365 Damsteé, J. S.: Nitrogen isotopic fractionation associated with growth on dinitrogen
366 gas and nitrate by cyanobacteria, *Limnol. Oceanogr.*, 54, 1403-1411,
367 <https://doi.org/10.4319/lo.2009.54.4.1403>, 2009.
- 368 Brandes, J. A. and Devol, A. H.: A global marine-fixed nitrogen isotopic budget:
369 Implications for Holocene nitrogen cycling, *Global Biogeochem. Cycles*, 16, 67-61-67-
370 14, <https://doi.org/10.1029/2001GB001856>, 2002.
- 371 Brunner, B., Contreras, S., Lehmann, M. F., Matantseva, O., Rollog, M., Kalvelage, T.,
372 Klockgether, G., Lavik, G., Jetten, M. S. M., Kartal, B., and Kuypers, M. M.: Nitrogen
373 isotope effects induced by anammox bacteria, *Proc. Natl. Acad. Sci. U.S.A.*, 110,
374 18994-18999, <https://doi.org/10.1073/pnas.1310488110>, 2013.
- 375 Carpenter, E. J., Harvey, H. R., Fry, B., and Capone, D. G.: Biogeochemical tracers of
376 the marine cyanobacterium *Trichodesmium*, *Deep Sea Res., Part I*, 44, 27-38,
377 [https://doi.org/10.1016/S0967-0637\(96\)00091-X](https://doi.org/10.1016/S0967-0637(96)00091-X), 1997.
- 378 Casciotti, K. L.: Nitrogen and oxygen isotopic studies of the marine nitrogen cycle,
379 *Ann Rev Mar Sci*, 8, 379-407, <https://doi.org/10.1146/annurev-marine-010213-135052>,
380 2016.
- 381 de Marsac, N. T. and Houmard, J.: [34] Complementary chromatic adaptation:
382 Physiological conditions and action spectra, in: *Methods Enzymol.*, Academic Press,



- 383 318-328, [https://doi.org/10.1016/0076-6879\(88\)67037-6](https://doi.org/10.1016/0076-6879(88)67037-6), 1988.
- 384 Eady, R. R.: Structure-function relationships of alternative nitrogenases, *Chem. Rev.*,
385 96, 3013-3030, <https://doi.org/10.1021/cr950057h>, 1996.
- 386 Foster, G. L., Royer, D. L., and Lunt, D. J.: Future climate forcing potentially without
387 precedent in the last 420 million years, *Nat. Commun.*, 8, 14845,
388 <https://doi.org/10.1038/ncomms14845>, 2017.
- 389 Giordano, M., Beardall, J., and Raven, J. A.: CO₂ concentrating mechanisms in algae:
390 Mechanisms, environmental modulation, and evolution, *Annu. Rev. Plant Biol.*, 56, 99-
391 131, <https://doi.org/10.1146/annurev.arplant.56.032604.144052>, 2005.
- 392 Gruber, N. and Galloway, J. N.: An Earth-system perspective of the global nitrogen
393 cycle, *Nature*, 451, 293-296, <https://doi.org/10.1038/nature06592>, 2008.
- 394 Guth, J. H. and Burris, R. H.: Inhibition of nitrogenase-catalyzed ammonia formation
395 by hydrogen, *Biochemistry-U.S.*, 22, 5111-5122, <https://doi.org/10.1021/bi00291a010>,
396 1983.
- 397 Hadfield, K. L. and Bulen, W. A.: Adenosine triphosphate requirement of nitrogenase
398 from *Azotobacter vinelandii*, *Biochemistry-U.S.*, 8, 5103-5108,
399 <https://doi.org/10.1021/bi00840a064>, 1969.
- 400 Hong, H., Shen, R., Zhang, F., Wen, Z., Chang, S., Lin, W., Kranz, S. A., Luo, Y., Kao,
401 S. J., Morel, F. M. M., and Shi, D.: The complex effects of ocean acidification on the
402 prominent N₂-fixing cyanobacterium *Trichodesmium*, *Science*, 356, 527-531,
403 <https://doi.org/10.1126/science.aal2981>, 2017.
- 404 Hönisch, B., Ridgwell, A. J., Schmidt, D. N., Thomas, E., Gibbs, S. J., Sluijs, A., R.,
405 Z., Kump, L., Martindale, R. C., Greene, S. E., Kiessling, W., Ries, J., Zachos, J. C.,
406 Royer, D., Barker, S., Marchitto Jr, T. M., Moyer, R., Pelejero, C., Ziveri, P., Foster, G.
407 L., and Williams, B.: The geological record of ocean acidification, *Science*, 335, 1058-
408 1063, <https://doi.org/10.1126/science.12082>, 2012.
- 409 Imam, S. and Eady, R. R.: Nitrogenase of *Klebsiella pneumoniae*: reductant-
410 independent ATP hydrolysis and the effect of pH on the efficiency of coupling of ATP
411 hydrolysis to substrate reduction, *FEBS Lett.*, 110, 35-38, [https://doi.org/10.1016/0014-
412 5793\(80\)80016-0](https://doi.org/10.1016/0014-5793(80)80016-0), 1980.
- 413 Kaplan, A. and Reinhold, L.: CO₂ concentrating mechanisms in photosynthetic
414 microorganisms, *Annu. Rev. Plant Physiol. Plant Mol. Biol.*, 50, 539-570,
415 <https://doi.org/10.1146/annurev.arplant.50.1.539>, 1999.
- 416 Kranz, S. A., Eichner, M., and Rost, B.: Interactions between CCM and N₂ fixation in
417 *Trichodesmium*, *Photosynthesis Research*, 109, 73-84, [https://doi.org/10.1007/s1120-
418 010-9611-3](https://doi.org/10.1007/s1120-010-9611-3), 2011.



- 419 Kranz, S. A., Sültemeyer, D., Richter, K. U., and Rost, B.: Carbon acquisition by
420 *Trichodesmium*: The effect of pCO₂ and diurnal changes, *Limnol. Oceanogr.*, 54, 548–
421 559, <https://doi.org/10.4319/lo.2009.54.2.0548>, 2009.
- 422 Levitan, O., Rosenberg, G., Setlik, I., Setlikova, E., Grigel, J., Klepetar, J., Prasil, O.,
423 and Berman-Frank, I.: Elevated CO₂ enhances nitrogen fixation and growth in the
424 marine cyanobacterium *Trichodesmium*, *Global Change Biol.*, 13, 531-538,
425 <https://doi.org/10.1111/j.1365-2486.2006.01314.x>, 2007.
- 426 Li, C., Jian, Z., Jia, G., Dang, H., and Wang, J.: Nitrogen fixation changes regulated by
427 upper water structure in the South China Sea during the last two glacial cycles, *Global*
428 *Biogeochem. Cycles*, 33, 1010-1025, <https://doi.org/10.1029/2019gb006262>, 2019.
- 429 Lloyd, M. K., McClelland, H. L. O., Antler, G., Bradley, A. S., Halevy, I., Junium, C.
430 K., Wankel, S. D., and Zerkle, A. L.: The isotopic imprint of life on an evolving planet,
431 *Space Sci. Rev.*, 216, <https://doi.org/10.1007/s11214-020-00730-6>, 2020.
- 432 McRose, D. L., Lee, A., Kopf, S. H., Baars, O., Kraepiel, A. M. L., Sigman, D. M.,
433 Morel, F. M. M., and Zhang, X.: Effect of iron limitation on the isotopic composition
434 of cellular and released fixed nitrogen in *Azotobacter vinelandii*, *Geochim. Cosmochim.*
435 *Acta*, 244, 12-23, <https://doi.org/10.1016/j.gca.2018.09.023>, 2019.
- 436 Miller, R. W. and Eady, R. R.: Molybdenum and vanadium nitrogenases of *Azotobacter*
437 *Chroococcum*: Low temperature favors N₂ reduction by vanadium nitrogenase,
438 *Biochem. J.*, 256, 429-432, <https://doi.org/10.1042/bj2560429>, 1988.
- 439 Minagawa, M. and Wada, E.: Nitrogen isotope ratios of red tide organisms in the East
440 China Sea: A characterization of biological nitrogen fixation, *Mar. Chem.*, 19, 245-259,
441 [https://doi.org/10.1016/0304-4203\(86\)90026-5](https://doi.org/10.1016/0304-4203(86)90026-5), 1986.
- 442 Mohr, W., Großkopf, T., Wallace, D. W., and LaRoche, J.: Methodological
443 underestimation of oceanic nitrogen fixation rates, *PLoS One*, 5, e12583,
444 <https://doi.org/10.1371/journal.pone.0012583.g001>, 2010.
- 445 Montoya, J. P.: Chapter 29 - Nitrogen stable isotopes in marine environments, in:
446 *Nitrogen in the Marine Environment (Second Edition)*, edited by: Capone, D. G., Bronk,
447 D. A., Mulholland, M. R., and Carpenter, E. J., Academic Press, San Diego, 1277-1302,
448 <https://doi.org/10.1016/B978-0-12-372522-6.00029-3>, 2008.
- 449 Montoya, J. P., Voss, M., Kähler, P., and Capone, D. G.: A simple, high-precision, high-
450 sensitivity tracer assay for N₂ fixation, *Appl. Environ. Microbiol.*, 62, 986-993,
451 <https://doi.org/10.1128/AEM.62.3.986-993.1996>, 1996.
- 452 Pham, D. N. and Burgess, B. K.: Nitrogenase reactivity: effects of pH on substrate
453 reduction and CO inhibition, *Biochemistry-US*, 32, 13725-13731,
454 <https://doi.org/10.1021/bi00212a043>, 1993.



- 455 Pierrot, D., Wallace, D. W. R., Lewis, E. R., Pierrot, D., Wallace, R., Wallace, D. W. R.,
456 and Wallace, W. E.: MS excel program developed for CO₂ system calculations, 2011.
- 457 Ren, H., Sigman, D. M., Meckler, A. N., Plessen, B., Robinson, R. S., Rosenthal, Y.,
458 and Haug, G. H.: Foraminiferal isotope evidence of reduced nitrogen fixation in the ice
459 age Atlantic Ocean, *Science*, 323, 244-248, <https://doi.org/10.1126/science.1165787>,
460 2009.
- 461 Rowell, P., James, W., Smith, W. L., Handley, L. L., and M., S. C.: ¹⁵N discrimination
462 in molybdenum- and vanadium-grown N₂-fixing *Anabaena Variabilis* and *Azotobacter*
463 *Vinelandii*, *Soil Biol. Biochem.*, 31, 2177-2180, [https://doi.org/10.1016/S0038-](https://doi.org/10.1016/S0038-0717(98)00066-2)
464 [0717\(98\)00066-2](https://doi.org/10.1016/S0038-0717(98)00066-2), 1998.
- 465 Schneider, K., Müller, A., Krahn, E., Hagen, W. R., Wassink, H., and Knüttel, K. H.:
466 The molybdenum nitrogenase from wild-type *Xanthobacter autotrophicus* exhibits
467 properties reminiscent of alternative nitrogenases, *Eur. J. Biochem.*, 230, 666-675,
468 <https://doi.org/10.1111/j.1432-1033.1995.0666h.x>, 1995.
- 469 Shen, Y., Pinti, D. L., and Hashizume, K.: Biogeochemical cycles of sulfur and nitrogen
470 in the Archean ocean and atmosphere, in: Archean Geodynamics and Environments,
471 305-320, <https://doi.org/10.1029/164GM19>, 2006.
- 472 Shi, D., Xu, Y., and Morel, F. M. M.: Effects of the pH/CO₂ control method on medium
473 chemistry and phytoplankton growth, *Biogeosciences*, 6, 1199-1207,
474 <https://doi.org/10.5194/bg-6-1199-2009>, 2009.
- 475 Shi, D. L., Kranz, S. A., Kim, J.-M., and morel, F. M. M.: Ocean acidification slows
476 nitrogen fixation and growth in the dominant diazotroph *Trichodesmium* under low-
477 iron conditions, *Proc. Natl. Acad. Sci. U.S.A.*, 109, E3094-E3100,
478 <https://doi.org/10.1073/pnas.1216012109>, 2012.
- 479 Sigman, D. M., DiFiore, P. J., Hain, M. P., Deutsch, C., Wang, Y., Karl, D. M., Knapp,
480 A. N., Lehmann, M. F., and Pantoja, S.: The dual isotopes of deep nitrate as a constraint
481 on the cycle and budget of oceanic fixed nitrogen, *Deep Sea Res., Part I*, 56, 1419-1439,
482 <https://doi.org/10.1016/j.dsr.2009.04.007>, 2009.
- 483 Silverman, S. N., Kopf, S. H., Bebout, B. M., Gordon, R., and Som, S. M.:
484 Morphological and isotopic changes of heterocystous cyanobacteria in response to N₂
485 partial pressure, *Geobiology*, 17, 60-75, <https://doi.org/10.1111/gbi.12312>, 2019.
- 486 Straub, M., Sigman, D. M., Ren, H., Martínez-García, A., Meckler, A. N., Hain, M. P.,
487 and Haug, G. H.: Changes in North Atlantic nitrogen fixation controlled by ocean
488 circulation, *Nature*, 501, 200-203, <https://doi.org/10.1038/nature12397>, 2013.
- 489 Stueken, E. E., Buick, R., Guy, B. M., and Koehler, M. C.: Isotopic evidence for
490 biological nitrogen fixation by molybdenum-nitrogenase from 3.2 Gyr, *Nature*, 520,
491 666-669, <https://doi.org/10.1038/nature14180>, 2015.



- 492 Sunda, W. G., Price, N. M., and Morel, F. M. M.: Trace metal ion buffers and their use
493 in culture studies, in: *Algal Culturing Techniques*, Academic Press, Burlington, MA,
494 35-63, <https://doi.org/10.1016/B978-012088426-1/50005-6>, 2005.
- 495 Wen, Z., Browning, T. J., Cai, Y., Dai, R., Zhang, R., Du, C., Jiang, R., Lin, W., Liu, X.,
496 Cao, Z., Hong, H., Dai, M., and Shi, D.: Nutrient regulation of biological nitrogen
497 fixation across the tropical western North Pacific, *Sci. Adv.*, 8, eabl7564,
498 <https://doi.org/10.1126/sciadv.abl7564>, 2022.
- 499 Yang, Z.-Y., Khadka, N., Lukoyanov, D., Hoffman, B. M., Dean, D. R., and Seefeldt,
500 L. C.: On reversible H₂ loss upon N₂ binding to FeMo-cofactor of nitrogenase, *Proc.*
501 *Natl. Acad. Sci. U.S.A.*, 110, 16327-16332, <https://doi.org/10.1073/pnas.1315852110>,
502 2013.
- 503 Zerkle, A. L., Junium, C. K., Canfield, D. E., and House, C. H.: Production of ¹⁵N-
504 depleted biomass during cyanobacterial N₂-fixation at high Fe concentrations, *J.*
505 *Geophys. Res.*, 113, <https://doi.org/10.1029/2007jg000651>, 2008.
- 506 Zhang, F., Hong, H., Kranz, S. A., Shen, R., Lin, W., and Shi, D.: Proteomic responses
507 to ocean acidification of the marine diazotroph *Trichodesmium* under iron-replete and
508 iron-limited conditions, *Photosynth. Res.*, 142, 17-34, [https://doi.org/10.1007/s11120-
509 019-00643-8](https://doi.org/10.1007/s11120-019-00643-8), 2019.
- 510 Zhang, F., Wen, Z., Wang, S., Tang, W., Luo, Y.-W., Kranz, S. A., Hong, H., and Shi,
511 D.: Phosphate limitation intensifies negative effects of ocean acidification on globally
512 important nitrogen fixing cyanobacterium, *Nat. Commun.*, 13, 6730,
513 <https://doi.org/10.1038/s41467-022-34586-x>, 2022.
- 514 Zhang, H. and Byrne, R. H.: Spectrophotometric pH measurements of surface seawater
515 at in-situ conditions: Absorbance and protonation behavior of thymol blue, *Mar. Chem.*,
516 52, 17-25, <https://doi.org/10.1016/j.aca.2019.06.024>, 1996.
- 517 Zhang, X., Sigman, D. M., Morel, F. M. M., and Kraepiel, A. M. L.: Nitrogen isotope
518 fractionation by alternative nitrogenases and past ocean anoxia, *Proc. Natl. Acad. Sci.*
519 *U.S.A.*, 111, 4782-4787, <https://doi.org/10.1073/pnas.1402976111>, 2014.
- 520